Three color coherent generation and control of current in low-temperature-grown GaAs

J. M. Fraser, A. Haché,[a] A. I. Shkrebtii, J. E. Sipe, and H. M. van Driel[b]
Department of Physics, University of Toronto, Toronto, Canada, M5S-1A7

(Received 11 December 1998; accepted for publication 10 February 1999)

We demonstrate coherent generation and control of electrical currents in low-temperature-grown GaAs at 300 K using three phase-related, 150 fs pulses derived from a parametric process. Interference between single photon (0.8 μm) and nondegenerate two photon (1.4 and 1.8 μm) absorption amplitudes generates ballistic electrical currents whose beam polarization dependence is in agreement with a simple Fermi's golden rule calculation. © *1999 American Institute of Physics.* [S0003-6951(99)01914-2]

The use of phased optical beams to control atoms, molecules,[1–4] and electrons in solids[5–11] via quantum interference processes has been widely investigated in recent years. Many demonstrations involve the interference of absorption pathways for harmonically related beams. For example, atomic populations have been controlled via interference of single and three photon absorption,[4] and electrical currents have been controlled in GaAs and low-temperature-grown (LT) GaAs[8–10] using single and two photon interband absorption processes. Here we illustrate the quantum interference control of electrical currents in LT-GaAs using three beams that are not harmonically related but are phase related since they are derived from a phase-matched optical parametric processes. Current injection occurs as a result of the interference of single photon absorption with nondegenerate two photon absorption pathways. The additional degree of freedom may allow for optimization of coherent control phenomena in future applications, e.g., via near-resonant intermediate states. Here we show that three colors allow one to separate the different elements of the current injection tensor. We also present calculations of the dispersion of the elements in clean GaAs (band gap, $E_g=1.42$ eV at 300 K).[12]

The formulation of the three color problem is a simple extension of the two color process.[8] For three beams the current density $\mathbf{J}_{e,h}$ for electrons (e) and holes (h) is given by:

$$\frac{dJ^a_{e(h)}}{dt}=\eta^{abcd}_{e(h)}(\omega_3,\Delta)E^b(-\omega_1)E^c(-\omega_2)E^d(\omega_3)+\text{c.c.}, \tag{1}$$

where $E(\cdots)$ designates the complex field amplitude[13] inside the sample, $\Delta\equiv\omega_2-\omega_1$, and $\omega_3=\omega_1+\omega_2$; superscripts indicate Cartesian components. Momentum relaxation of carriers can be included phenomenologically by adding a term $-J^a_{e(h)}/\tau_{e(h)}$ to the right hand side of Eq. (1), where $\tau_{e(h)}$ is the appropriate relaxation time. The total current injection tensor is given by $\eta^{abcd}(\omega_3,\Delta)\equiv\eta^{abcd}_e(\omega_3,\Delta)+\eta^{abcd}_h(\omega_3,\Delta)$; generally $|\eta^{abcd}_e(\omega_3,\Delta)|\gg|\eta^{abcd}_h(\omega_3,\Delta)|$, because of the lighter effective mass of the electrons, but typically both η_e and η_h, which are purely imaginary, have the same sign. For crystalline GaAs, the only nonzero elements of the η tensor are *xxxx*, *xxyy*, *xyxy*, *xyyx*, and related elements by *x*, *y*, and *z* exchange.[14] The tensor is a measure of the polarity of the electron distribution created by the interference of single (ω_3) and two photon ($\omega_1+\omega_2$) processes. Note that degenerate two photon absorption can also occur for one or both of the ω_1 and ω_2 beams alone if $\hbar\omega_1$ or $\hbar\omega_2>E_g/2$. Since these processes access different initial and final states than those accessed by the ω_3 beam they do not contribute to the interference effect. For a particular tensor element, e.g., the *xxyy* element, Eq. (1) explicitly becomes:

$$\frac{dJ^x}{dt}=-2\,\text{Im}\,\eta^{xxyy}(\omega_3,\Delta)|E^x(\omega_1)|\times|E^y(\omega_2)||E^y(\omega_3)|\sin(\phi_3-\phi_2-\phi_1), \tag{2}$$

where the phases ϕ_α are defined according to $E^a(\omega_\alpha)=|E^a(\omega_\alpha)|e^{i\phi_\alpha}$; the phase parameter $\Delta\phi\equiv\phi_3-\phi_1-\phi_2$ can be used to control the current direction and magnitude.

By following Atansov *et al.*[8] and assuming that ω_3 is the only resonant frequency with $\hbar\omega_1$ and $\hbar\omega_2<E_g$ we find:

$$\eta^{abcd}_{e(h)}(\omega_3,\Delta)=\frac{-(+)2\pi ie^4}{\hbar^3\omega_1\omega_2\omega_3}\sum_{c,v,n}\int\frac{d\mathbf{k}}{8\pi^3}v^a_{cc(vv)}\times\left[\frac{v^b_{nc}v^c_{vn}}{\overline{\omega}_{cv}-\omega_n+(\Delta/2)}+\frac{v^c_{nc}v^b_{vn}}{\overline{\omega}_{cv}-\omega_n-(\Delta/2)}\right]v^d_{cv}\delta(\omega_{cv}-\omega_3), \tag{3}$$

where $\omega_{cv}(\mathbf{k})\equiv\omega_c(\mathbf{k})-\omega_v(\mathbf{k})$, $\overline{\omega}_{cv}(\mathbf{k})\equiv[\omega_c(\mathbf{k})+\omega_v(\mathbf{k})]/2$, $\mathbf{v}_{nc}(\mathbf{k})$ denotes the matrix element of the velocity operator between bands n and c, the subscripts c and v refer, respectively, to conduction and valence bands, and n denotes a band of either type; the $\mathbf{k}$ dependence of these quantities in Eq. (3) has been kept implicit. We here sum explicitly over bands with different spins. In the degenerate limit ($\Delta=0$) $\eta^{abcd}_{e(h)}(2\omega;0)=2\,\eta^{abcd}_{e(h)}(2\omega)$, where $\eta^{abcd}_{e(h)}(2\omega)$ is the result of Atanasov *et al.*;[8] this is as it should be.[15]

[a]Permanent address: Département de Physique, Université de Moncton, Moncton, NB E1A 3E9, Canada.
[b]Electronic mail: vandriel@physics.utoronto.ca

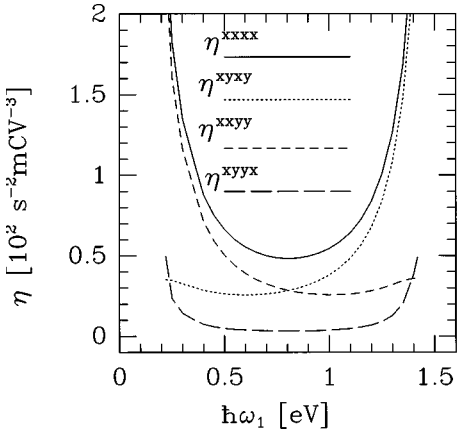

FIG. 1. Dispersion in the current injection tensor elements associated with GaAs. For comparison with experimental results we choose $\hbar\omega_3 = 1.55$ eV; the abscissa is $\hbar\omega_1$, with $\omega_1+\omega_2=\omega_3$.

Returning to the nondegenerate case, when $\Delta>0$ the first term in square brackets in Eq. (3) ''enhances'' the contribution from the intermediate conduction (virtual electron) states with respect to the degenerate case ($\Delta=0$), but ''suppresses'' the virtual hole contribution. The roles of virtual electron and hole terms are reversed in the second term in square brackets in Eq. (3). The divergences as $\Delta\rightarrow\pm\omega_3$ are associated with either the ω_1 or ω_2 beam becoming resonant with the band gap, and the *intraband* motion of the injected electrons and holes is also resonantly driven. For nonzero Δ the expression (3) indicates a difference in $\eta^{xxyy}(\omega_3,\Delta)$ and $\eta^{xyxy}(\omega_3,\Delta)$ but with $\eta^{xxyy}(\omega_3,\Delta)=\eta^{xyxy}(\omega_3,-\Delta)$.

Figure 1 shows the calculated four nonzero tensor elements for GaAs as a function of ω_1 over the range $|\hbar\Delta| < 2E_g-\hbar\omega_3$, with $\hbar\omega_3=1.55$ eV (0.8 μm). To calculate the wave functions and eigenenergies we employed a pseudopotential plane wave approach, a modification of a molecular dynamics program.[16] The nonlocal pseudopotential of Hamann[17,18] forms the basis of the electronic structure calculation; we used the local density approximation (LDA) exchange-correlation potential as parameterized by Perdew and Zunger.[19] To correct for the LDA band gap, self-energy corrections were included at the level of the ''scissors'' approximation, modifying the velocity matrix elements as proposed by Levine *et al.*[20] Spin-orbit effects are neglected. The irreducible Brillouin zone was sampled with a hybrid tetrahedron-random sampling method[21] with >1300 points.

Note that in the ''*xxxx*'' geometry the minimum current injection occurs under conditions of degeneracy ($\omega_1=\omega_2$), as does the minimum two photon absorption;[22] but the minimum here is much shallower than in two photon absorption. Under conditions of nondegeneracy the *xyxy* and *xxyy* components are distinguishable. This can be understood qualitatively since the larger component occurs when the nonresonant beam with frequency closer to ω_3 is also polarized in the same direction.

The experimental setup to observe three-color coherent control is shown in Fig. 2. High intensity ultrashort light pulses are used to maximize the nonlinear current generation while minimizing thermal effects. A regenerative amplified Ti:sapphire laser (0.8 μm) operating at a repetition rate of 250 kHz is used to pump an optical parametric amplifier to

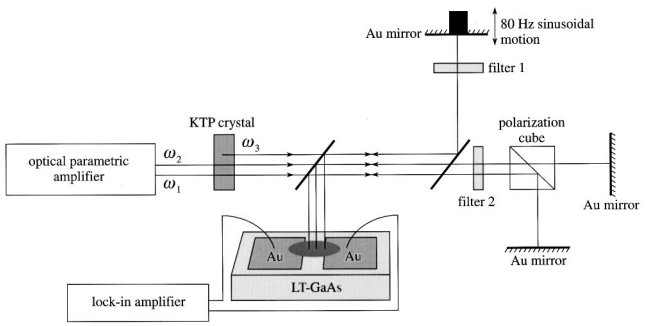

FIG. 2. Experimental setup. For the purposes of clarity, focusing optics are omitted and overlapped beams are shown spatially separated. Beams reflected from gold mirrors are directed slightly downward to be intercepted by a pick-off mirror and sent to the sample.

produce orthogonally polarized 150 fs pulses with 1.80 (ω_1) and 1.44 μm (ω_2) and average power of 1 to 2 mW. A phase-locked beam at 0.80 μm (ω_3) is produced by sum-frequency mixing in a 1.5-mm-thick $KTiPO_4$ crystal, however the beam from the Ti:sapphire laser can also be used. The three colors are separated into independent delay lines for individual control of pulse delay to maximize temporal overlap. One delay line (ω_3) is mounted on a piezoelectric actuator to allow fine control of $\Delta\phi$.

The semiconductor is a 1 μm epilayer of annealed, low-temperature-grown GaAs (resistivity $\sim 10^7\ \Omega$ cm) on a substrate of (001) GaAs. The three beams are focused to provide beam waists ranging from 60 to 90 μm, yielding peak irradiances of 0.6, 1.4, and 15 MW/cm^2 for ω_1, ω_2, and ω_3, respectively. Peak carrier density is on the order of 1×10^{17} cm^{-3}. To observe the ultrafast signals, we integrate the current by collecting charges on unbiased gold electrodes separated by a 10 μm gap.[9] The crystal/electrodes are configured so as to make the (100) crystal direction across the gap with the (010) direction along the gap allowing us to make use of the η^{xxyy} tensor. The fast trapping time of the LT-GaAs causes the sample to return to high resistivity on a picosecond time scale thus minimizing carrier discharge through the sample.[10] The electrodes are connected directly to a lock-in amplifier (100 MΩ input impedance). The measured steady-state voltage signal corresponds to the integrated current, i.e., total collected charge, discharging through the lock-in amplifier. Phase mismatch of the three beams due to material dispersion[10] is not an important consideration in this experiment due to the relatively short attenuation depth (1.5 μm)[23] of the ω_3 electric field. Background free measurements are performed by dithering $\Delta\phi$ about a given value at 80 Hz while using lock-in amplification.

The inset to Fig. 3 shows that the steady-state voltage has the expected dependence on $\Delta\phi$. The variation of current injection with the ω_3 irradiance, $I(\omega_3)$, was determined from 60 kW cm^{-2} to 15 MW cm^{-2} while both the ω_1 and ω_2 beam peak irradiances were held constant. Results are shown in the main part of Fig. 3. A best fit indicates that the current varies as $I(\omega_3)^{0.45\pm0.03}$, close to the $I(\omega_3)^{0.5}$ dependence expected theoretically (albeit, for the current injection rate). By rotating the sample 90° along with the polarization of the ω_3 beam, we can access the η^{xyxy} tensor element. The magnitude of the injected current then decreases by ~30% in ap-

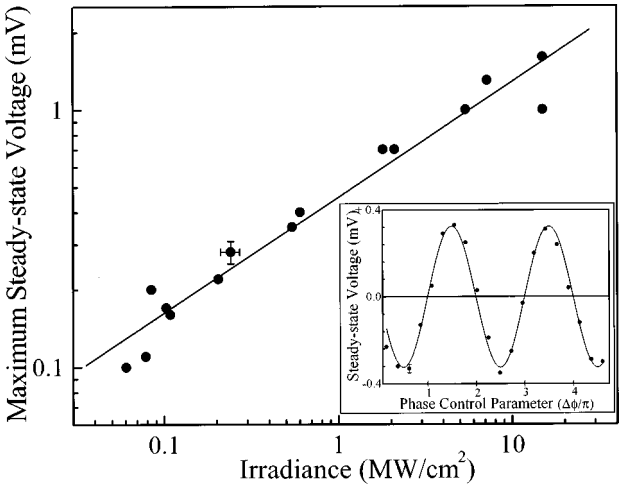

FIG. 3. Dependence of maximum steady state voltage on ω_3 beam irradiance. Solid line is the best fit to a power law with exponent 0.45 ± 0.03. Inset: Collected charge amplitude as a function of the phase control parameter between three-color beams of 1.44, 1.80, and 0.80 μm. The solid curve is a best fit to the data assuming a sinusoidal shape.

proximate agreement with the theoretical results of Fig. 1. A more detailed analysis of the momentum relaxation and the dynamics of the circuit would be required to effect a more quantitative comparison of theory with experiment; nonetheless, this difference is observed to vanish as $\omega_1 \rightarrow \omega_2$, in agreement with theory.

In conclusion, we have demonstrated that the coherent control of photocurrents in semiconductors can occur using phase-related, but not harmonically related optical beams. This offers an additional degree of freedom to enhance coherence control processes in general. In the case of current generation in semiconductors, such an enhancement can occur as $\hbar\omega_1$ or $\hbar\omega_2$ approach an intermediate resonance such as an impurity level, or even the band gap as Fig. 1 illustrates. More detailed considerations would have to take into account the width of the pulses and their spectral content under such near-resonant conditions. Using the nondegenerate beams we have verified the difference of two elements of the current injection tensor that are the same under degenerate conditions.

The authors gratefully acknowledge financial support from the Natural Sciences and Engineering Research Council of Canada and Photonics Research Ontario. J.M.F. acknowledges additional support from the Walter C. Sumner Foundation and HMvD is thankful for a Killam Fellowship from the Canada Council.

[1] P. Brumer and M. Shapiro, Acc. Chem. Res. **22**, 407 (1989).
[2] W. S. Warren, H. Rabitz, and M. Daleh, Science **259**, 1581 (1993).
[3] M. O. Scully and S.-Y. Zhu, Science **281**, 1973 (1998).
[4] C. Chen, Y.-Y. Yin, and D. S. Elliot, Phys. Rev. Lett. **64**, 507 (1990).
[5] B. Ya. Zel'dovich and A. N. Chudinov, Pis'ma Zh. Eksp. Teor. Fiz. **50**, 409 (1989).
[6] A. P. Heberle, J. J. Baumberg, and K. Kohler, Phys. Rev. Lett. **75**, 2598 (1995).
[7] E. Dupont, P. B. Corkum, H. C. Liu, M. Buchanan, and Z. R. Wasilewski, Phys. Rev. Lett. **74**, 3596 (1995).
[8] R. Atanasov, A. Haché, J. L. P. Hughes, H. M. van Driel, and J. E. Sipe, Phys. Rev. Lett. **76**, 1703 (1996).
[9] A. Haché, Y. Kostoulas, R. Atanasov, J. L. P. Hughes, J. E. Sipe, and H. M. van Driel, Phys. Rev. Lett. **78**, 306 (1997).
[10] A. Haché, J. E. Sipe, and H. M. van Driel, IEEE J. Quantum Electron. **35**, 1144 (1998).
[11] W. Pötz, Phys. Rev. Lett. **79**, 3262 (1997).
[12] *Semiconductors—Basic Data*, edited by O. Madelung (Springer, Berlin, 1996).
[13] The monochromatic field amplitudes are defined via $E(t)=E(\omega)\times\exp(-i\omega t)+\text{c.c.}$
[14] For example, see P. N. Butcher and D. Cotter, *The Elements of Nonlinear Optics* (Cambridge University Press, Cambridge, U.K., 1990).
[15] Note that in the degenerate case (ω_1, $\omega_2 \rightarrow \omega$, $\omega_3 \rightarrow 2\omega$) we can take $\mathbf{E}(\omega_1) \rightarrow f^*\mathbf{E}(\omega)$, $\mathbf{E}(\omega_2) \rightarrow (1-f^*)\mathbf{E}(\omega)$, where $\mathbf{E}(\omega)[=\mathbf{E}(\omega_1)+\mathbf{E}(\omega_2)]$ is the total amplitude at ω and f is any complex number. When that limit is reached we must take into account the fact that the degenerate two photon absorption processes involving $\omega_1+\omega_1$ and $\omega_2+\omega_2$ also connect the same initial and final states as the one photon absorption at $\omega_3=2\omega$, so our total current injection is then $dJ^a_{e(h)}/dt = \eta^{abcd}_{e(h)}(2\omega;0)f(1-f)E^b(-\omega)E^c(-\omega)E^d(2\omega) + \eta^{abcd}_{e(h)}(2\omega)f^2E^b(-\omega)E^c(-\omega)E^d(2\omega) + \eta^{abcd}_{e(h)}(2\omega)(1-f)^2E^b(-\omega)E^c(-\omega)E^d(2\omega)+cc$. Since $\eta^{abcd}_{e(h)}(2\omega;0)=2\eta^{abcd}_{e(h)}(2\omega)$ this equals $\eta^{abcd}_{e(h)}(2\omega)E^b(-\omega)E^c(-\omega)E^d(2\omega)+cc.$, in agreement with Atanasov *et al.* (Ref. 8).
[16] M. Bockstedte, A. Kley, J. Neugebauer, and M. Scheffler, Comput. Phys. Commun. **107**, 187 (1997).
[17] D. R. Hamann, Phys. Rev. B **40**, 2980 (1989).
[18] M. Fuchs, M. Bockstedte, and M. Scheffler (private communication).
[19] J. P. Perdew and A. Zunger, Phys. Rev. B **23**, 5048 (1981).
[20] Z. Levine and D. Allan, Phys. Rev. Lett. **63**, 1719 (1989).
[21] J. L. P. Hughes and J. E. Sipe, Phys. Rev. B **54**, 10751 (1996).
[22] D. C. Hutchings and E. W. Van Stryland, J. Opt. Soc. Am. B **9**, 2065 (1992).
[23] *Handbook of Optical Constants of Solids*, edited by E. D. Palik (Academic, Orlando, Fl, 1985).